Proc. Indian Acad. Sci. (*Chem. Sci.*), Vol. 114, No. 6, December 2002, pp 579–592

Protein scissors: Photocleavage of proteins at specific locations

CHALLA V KUMAR*,[1], APINYA BURANAPRAPUK[2] and JYOTSNA THOTA[1]
[1]Department of Chemistry, University of Connecticut, Storrs, CT 06269-3060, USA
[2]Department of Chemistry, Srinakharinwirot University, Sukhumvit 23, Bangkok 10110, Thailand
e-mail: cvkumar@nucleus.chem.uconn.edu

Abstract. Site-specific photocleavage of hen egg lysozyme and bovine serum albumin (BSA) by N-(L-phenylalanine)-4(1-pyrene)butyramide (Py-Phe) is investigated in detail with respect to its efficiency, dependence on oxygen, and radical quenchers. Binding of Py-Phe to BSA follows a biphasic process with two binding sites per protein. The photocleavage was achieved upon irradiating a mixture of protein, Py-Phe and Co(III)hexammine (CoHA) at 344 nm. No protein cleavage was observed in the absence of Py-Phe, or CoHA, or light. Photocleavage of BSA was inhibited by degassing or by the addition of radical quenchers such as ethanol. In addition, the photoreaction was quenched by electron donors such as ethanolamine. This result was corroborated by the flash photolysis studies where the cation radical derived from the probe is also quenched by ethanolamine with an equivalent rate constant. Quenching of the singlet excited state of Py-Phe by CoHA followed by the reaction of the resulting pyrenyl cation radical with the protein backbone is the suggested mechanism of protein cleavage. The origin of the specificity of photocleavage is discussed and specificity is valuable in targeting desired sites of proteins with small molecules.

Keywords. Photocleavage; serum albumin; lysozyme; fluorescence; gelelectrophoresis.

1. Introduction

The binding of small molecules (ligands) to proteins is an important event in many biological processes.[1] Yet, the binding sites of many ligands and their binding dynamics remain largely unknown. One strategy to locate ligand binding sites on proteins is to attach a photochemical reagent to the ligand such that photoactivation of the reagent cleaves the protein at the ligand binding site. Such an approach requires the design of photochemical reagents that are capable of cleaving proteins at specific sites (photochemical proteases, chart 1). Several such reagents are reported from this laboratory in the past few years.[2–6]

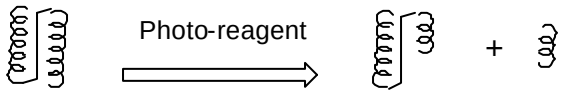

Chart 1. Site-specific photocleavage of proteins.

*For correspondence

Reagents that can cleave the protein backbone, on demand, are also useful[7–12] in the elucidation of protein structure. There are thousands of proteins whose structures are yet to be determined, and chemical methods that can provide structural information will be valuable. Chemical reagents that can cleave the membrane bound proteins, for example, at the solvent-exposed residues will be useful to identify the protein domains that are accessible to the aqueous environment. Protein cleavage reagents are also useful to target specific proteins for degradation under photochemical conditions for therapeutic purposes. Rapid proliferation of chemical nucleases for DNA cleavage studies illustrates how reagents based on small molecules are useful for the chemical manipulation of biomolecules.[12–16] Chemical proteases, analogously, are useful for biochemical applications.[7–12,16–20] Another important application can be in the chemical synthesis of novel proteins.

The current design of protein cleavage reagents combines the structural features that are needed for the recognition of the ligand binding site on a protein with the electronic properties necessary for the desired photochemical reactivity. Any such design of probes has to take into consideration the general structural aspects of proteins.[21] Most globular, water-soluble proteins display hydrophilic residues on the outside, and occasionally, some hydrophobic clefts.[22] Reagents that have a suitable chromophore which can bind in the hydrophobic clefts, for example, and make contacts with hydrophilic ionic head-groups on the out side are expected to show high affinities for these sites (chart 2). The binding of the reagent, further more, is to be restricted to one of such sites, if one desires to achieve specificity (100% selectivity) or high selectivity. Achieving specificity for photocleavage is important, but it is also challenging.[16–20]

High selectivity, therefore, was achieved by controlling the structural features of the reagent. The hydrophobic clefts present on a protein often differ in terms of their size, depth, and the type of residues that are present at the cavity-openings. By controlling the size of the hydrophobic segment, the charge on the head group, and its distance from the hydrophobic segment, high selectivity for binding is achieved (chart 2). Introduction of hydrogen bonding sites at specific locations, and incorporation of functionalities that can engage in residue-selective interactions at the binding site, such as salt-bridge formation, are additional strategies for improved selectivity. The binding, for example, can be directed to cavities whose openings are positively charged, by incorporating negatively charged head-groups (chart 2). Controlling the chirality of the head group also allows for considerable leverage in modulating the binding strength and chiral selectivity. Using such an approach the highest chiral selectivity (>1 : 100) for a non-natural ligand was achieved[6].

High binding selectivity, thus obtained by design, is then converted to high selectivity for protein cleavage by activating the protein-bound reagent under thermal or photo-

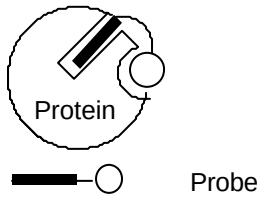

Chart 2. Binding of ligands to globular proteins at hydrophobic cavities while making specific contacts with polar residues at the binding site.

chemical conditions.[2–6,23] Use of light for protein cleavage has distinct advantages. Photoreactions are started and sustained with light, providing a sharp control for the initiation and termination of the reaction. Visible light is perhaps the least toxic reagent for environmentally responsible chemical approaches. Light initiated reactions are amenable for time-resolved studies to delineate the mechanism of the reaction.[4,5] By controlling the wavelength of excitation, specific chromophores are selectively activated to high energies, thereby minimizing side reactions. Visible light is a non-invasive reagent of low toxicity, and it is attractive for therapeutic applications.

New photochemical proteases are described here that have: (a) high affinities for selected sites on proteins; (b) strong absorption bands in the near visible region; (c) long-lived, singlet excited states that are convenient to initiate photoreactions; and a pyrenyl chromophore (Py) suitable for photoactivation (chart 3). Py has been used extensively to probe microenvironments in heterogeneous media, and considerable amount of literature exists on the photochemical properties of Py. Current studies focus on the use of a six-atom linker connecting the pyrenyl chromophore to L-phenylalanine. Phenylalanine is interesting due to its relevance in the binding and transport of hydrophobic amino acids or their metabolites by bovine serum albumin (BSA), in diseases such as phenylalanine ketonuria.[24] Py-Phe, developed in our laboratory, cleaves hen egg lysozyme, BSA, and carboxypeptidase A at a single site.[2–6]

Lysozyme and BSA are chosen for the current study to investigate the mechanistic details of the protein photocleavage. The crystal structure of lysozyme is known[25] and the enzymatic activity of lysozyme is useful to determine if the photoreaction damages key residues required for its activity. BSA is another appropriate protein for our studies as BSA is the most abundant protein in blood and BSA is considered as the primary protein that interacts with many drugs/pharmaceuticals. Hydrophobic ligands such as fatty acids, steroids, bilirubin, etc. are known to bind to serum albumin.[26] Because of its ability to bind and transport a variety of ligands, serum albumin is considered as an important biological target. The protein binding studies, and the mechanistic details of site-specific protein photocleavage are presented here.

2. Materials and methods

Lysozyme (MW = 14,300), bovine serum albumin (MW = 66,267), and lactoglobulin A (MW = 18,365) were purchased from Sigma Chemical Co. Protein solutions were prepared by dissolving the appropriate amount of the protein in 50 mM *Tris*-HCl, *p*H 7·0. Py-Phe, and the methyl ester of Py-Phe was synthesized as reported earlier.[2] The molar extinction coefficient of Py-Phe was estimated to be 42,600 M^{-1} cm^{-1} (343 nm). All probe solutions were prepared fresh, and they have been used within a day. Calibration graphs were constructed using Beer's law, and probe concentrations were restricted to the linear region of the graph. No excimer emission was observed in 0–50 *m*M range.

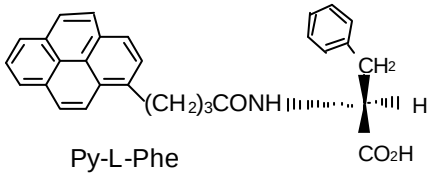

Chart 3. Structure of the chiral pyrenyl photoprobe.

2.1 *Photochemical protein cleavage*

Photocleavage reactions were carried out at room temperature in 50 mM *Tris*-HCl buffer, *p*H 7·0 unless noted otherwise. The mixtures of protein (15 *m*M) and Py-Phe (15 *m*M) in the presence of $Co(NH_3)_6Cl_3$, CoHA (1 mM) (total solution volume 100 *m*l) were irradiated at 344 nm (into the pyrenyl absorption band) using a 150 W xenon lamp source attached to a PTI model A1010 monochromator. UV cut-off filter (WG-345; 78% T at 344 nm) was used to remove stray UV light. Irradiated samples were evaporated to dryness for the gel electrophoresis experiments.

2.2 *SDS-gel electrophoresis*

SDS-PAGE experiments were performed as reported earlier.[27] Loading buffer (24 *m*l) (containing SDS (7% *w*/*v*), glycerol (4% w/v), *Tris* (50 mM), mercaptoethanol (2% *v*/*v*), Bromophenol blue (0·01% *w*/*v*, adjusted to *p*H 6·8 with HCl) was added to the dried protein samples. Protein solutions (8 µl) were aliquoted and heated for 3 min before loading on the gel. The gels were run by applying a voltage of 60 V, until the dye passed through the stacking gel, and the voltage was then increased to 110 V. The gels were run for a total time of 2·5 h for lysozyme, and 1·5 h for BSA. The gels were stained with Coomassie Blue for 4 h, and destained in acetic acid solution (10%) for 4 h. Bands in the gels were quantitated as reported earlier.[3,4]

2.3 *Spectroscopic methods*

All absorption spectra were recorded on a HP8453 diode array spectrophotometer, and all fluorescence spectra have been recorded on a Perkin-Elmer LS5B fluorimeter using software developed in this laboratory. The circular dichroism spectra were recorded on a JASCO J710 spectropolarimeter using software supplied from JASCO, and all spectral measurements have been carried out at room temperature.

3. Results

A series of chromophores linked to specific recognition elements via variable length tethers were designed, synthesized, and tested in our laboratory for their binding to proteins.[28–30] These probes bind avidly to globular proteins,[29,30] and longer tethers facilitated binding to proteins when compared to shorter analogs.[28,29] The details of the photocleavage properties of Py-Phe, containing a six-atom tether, are described here.

3.1 *Absorption studies*

The addition of a concentrated solution of BSA to Py-Phe (8·8 *m*M, 1 ml total, 1 cm path length) resulted in a decrease in absorbance at 343 nm. Plots of change in absorbance (ΔA) at 343 nm (closed circles, decrease in absorbance), and at 347 nm (open circles, increase in absorbance) are shown in figure 1a. The data are corrected for dilution, and BSA has no detectable absorbance in the 315–355 nm region. Both plots match in the low concentration regime (1 : 1 probe to protein concentrations) but deviated significantly at higher BSA concentrations. Such deviation suggests the presence of two distinct binding sites. Further increase in BSA concentration has no detectable effect, and the 347 nm peak, therefore, is assigned to the probe bound to a single site.[2]

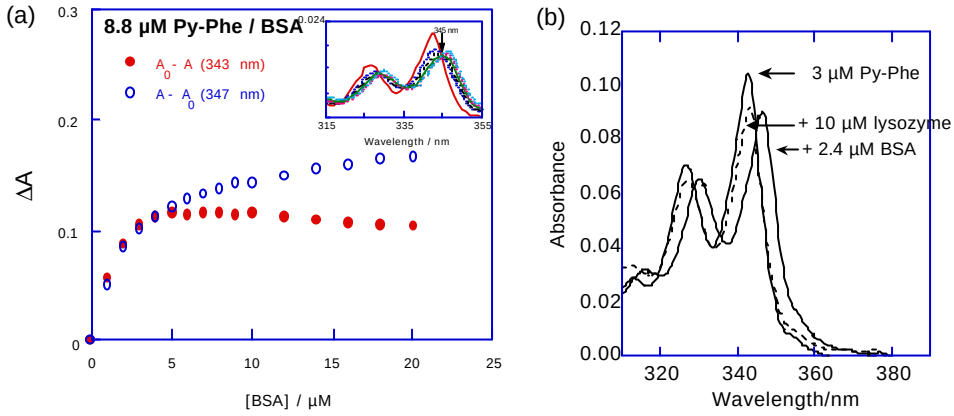

Figure 1. (**a**) Plots of the changes in the absorbance (ΔA) of Py-Phe (8·8 *m*M) as a function of BSA concentration (0–8 *m*M), observed at 343 and 347 nm. (**b**) Absorption spectra of Py-Phe (3 *m*M) in *Tris* buffer (50 mM *Tris* HCl, *p*H. 7·2), in the presence of BSA (2·4 *m*M), and in the presence of lysozyme (10 *m*M).

Table 1. Spectral properties of Py-Phe bound to BSA or lysozyme

Protein	Abs. max. (nm)	% Hyperchromism	Em. max. (nm)	$kq/10^{10}$ (M^{-1} s^{-1})
Buffer	343	0	376	1·7 ± 0·05
BSA	347	13	378	–
Lysozyme	343	12	378	1·2 ± 0·05

The absorption spectra recorded at increasing BSA concentrations are shown in figure 1a (inset). A sharp isosbestic point, wavelength where the absorbance is independent of the protein concentration, is present at 345 nm, indicating the presence of two spectroscopically distinguishable species. The absorption spectra of Py-Phe, recorded in the presence of BSA and in the presence of lysozyme, are compared in figure 1b. The corresponding peak positions and extinction coefficients are collected in table 1. While a red-shift of 4 nm was noted for BSA, only 1 nm shift is evident with lysozyme, but both proteins indicated hypochromism.

3.2 *Fluorescence studies*

Py-Phe fluoresces strongly upon excitation in the UV, and this prompted us to investigate Py-Phe binding using fluorescence methods. The fluorescence spectra of Py-Phe (2 *m*M) recorded in the buffer, in the presence of BSA (4 *m*M), and in the presence of lysozyme (10 *m*M) are shown in figure 2. The peak positions are essentially unchanged by the addition of protein solutions. The observed red-shift in the absorption spectrum of Py-Phe/BSA, and the lack of a significant, corresponding shift in the fluorescence spectra indicate that the Stoke's shift for the excited state in BSA is much smaller than that observed in the buffer (chart 4). The probe in BSA, therefore, is surrounded by the rigid

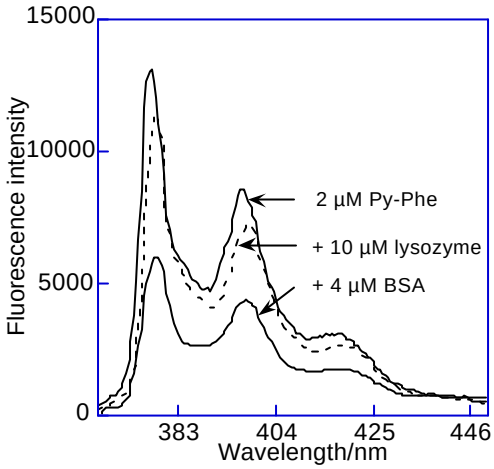

Figure 2. Fluorescence spectra of Py-Phe (2 *m*M, thick line, 345 nm excitation) in the presence of BSA (4 *m*M, thin line), and lysozyme (10 *m*M, dotted line).

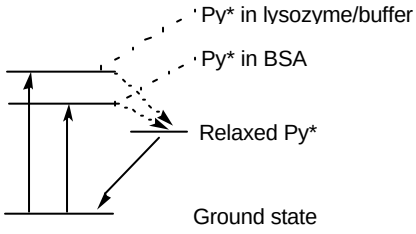

Chart 4. Energetics of Py* relaxation in BSA when compared to that in lysozyme or buffer.

protein matrix with little or no flexibility. The Stoke's shift estimated for Py-Phe bound to lysozyme is slightly larger than that of Py-Phe in buffer (table 1), and hence, the binding site in lysozyme is flexible or exposed to the solvent when compared to that in BSA.

3.3 *Fluorescence quenching studies*

Quenching of the pyrenyl excited state by CoHA is a prerequisite for the protein photocleavage. Steady state quenching experiments indicated that the protein matrix shields Py-Phe from the quencher, and BSA offers greater protection when compared to lysozyme.[3] Time-resolved fluorescence quenching experiments are conducted to probe the dynamics of quenching by CoHA. The fluorescence lifetimes of Py-Phe bound to the protein are measured in the presence of increasing concentrations of CoHA, and the corresponding quenching plots are shown in figure 3. The fluorescence lifetimes of Py-Phe/buffer and Py-Phe/lysozyme are quenched by CoHA with rate constants $1{\cdot}7 \pm 0{\cdot}05 \times 10^{10}$ M^{-1} s^{-1} and $1{\cdot}2 \pm 0{\cdot}05 \times 10^{10}$ M^{-1} s^{-1}, respectively (table 1). Fluorescence

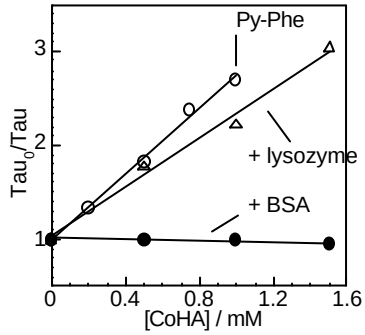

Figure 3. Quenching of the fluorescence lifetimes of Py-Phe (5 *m*M) by CoHA, in buffer (open circles), lysozyme (100 *m*M, triangles) and in the presence of BSA (20 *m*M, closed circles). The corresponding quenching rate constants are $1{\cdot}7 \times 10^{10}$ M^{-1} s^{-1}, and $1{\cdot}2 \times 10^{10}$ M^{-1} s^{-1}, respectively, while that of BSA is not quenched by CoHA.

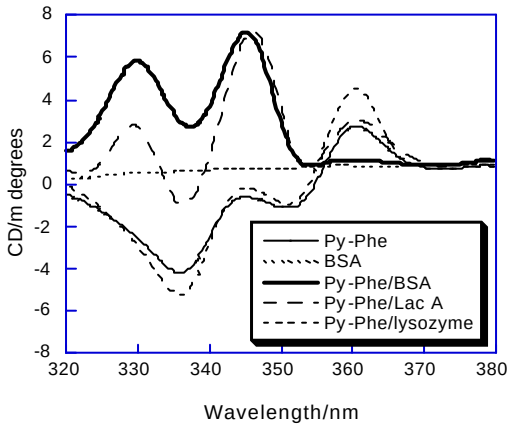

Figure 4. Circular dichroism spectra of Py-L-Phe (50 *m*M), in the presence of BSA (50 *m*M), in the presence of lysozyme (50 *m*M), and in the presence of lactoglobulin A (50 *m*M). No peaks were observed for proteins in this region (310–380 nm), in the absence of the probe.

lifetime of Py-Phe/BSA, in contrast, was not quenched by CoHA, but shows a small increase. This increase in emission is in contrast to the quenching reported in the steady-state data, and the increase is most likely due to changes in the protein conformation induced by the binding of CoHA to BSA.

3.4 *Circular dichroism (CD) studies*

The binding of ligands to asymmetric environments often results in induced CD (ICD). The strength, as well as the sign of ICD depends on the nature of the excitonic coupling between the probe and its asymmetric surroundings. The ICD spectra of Py-Phe (50 *m*M)

recorded in the presence of BSA, lysozyme, and lactoglobulin are shown in figure 4. The ICD spectrum recorded in the presence of lactoglobulin is a combination of the spectra obtained with BSA and lysozyme, and this is provided for comparison. The ICD spectrum changes significantly from protein to protein, and no two spectra are superimposable, and these provide a strong evidence that Py is in intimate contact with the asymmetric residues of the protein at the binding site.

3.5 *Protein cleavage studies*

Quenching of Py-Phe* by CoHA at the protein matrix results in rapid backbone cleavage, and the progress of the protein photocleavage was monitored in SDS-PAGE experiments. Photocleavage yield of BSA increases with irradiation time, and only two fragments of molecular weights (41 and 28 kDa) lower than that of the parent (68 kDa) are observed (5–18% yield, figure 5a, lane 6). If the photocleavage were to be random, one would have observed a smear, and molecular weights of the daughter fragments add up to that of the parent protein, within ± 1% error, consistent with a single cut in the protein backbone. Irradiation in the absence of CoHA, or in the absence of Py-Phe, or by keeping the sample in the dark did not yield any fragmentation.[4]

To determine the role of COOH function of Py-Phe in the recognition process, we have examined the photoreactivity of the corresponding methyl ester. The Py-Phe methyl ester does not induce photocleavage (figure 5a, lanes 2–5), while facile photocleavage was noted with Py-Phe, under the same experimental conditions (lane 6). Similarly, Py-Phe cleaves lysozyme at a single site (figure 5b, lane 6), but no photocleavage was observed with the methyl ester of Py-Phe (figure 5b, lanes 3, 4). Therefore, the carboxylate function of Py-Phe is important for the binding site recognition in BSA and lysozyme.

To investigate the role of the protein secondary and tertiary structure on the photocleavage reaction, we have examined the reactivity of heat-denatured BSA. (figure 5c) No photocleavage was observed for the denatured BSA, either in the presence or absence of Py-Phe, (lanes 4–7) while the native protein is cleaved by Py-Phe, as before (lane 8). Binding of Py-Phe to the native structure is essential for the observed photocleavage, and this fact high lights access to specific reactive sites on the protein that are responsible for the photocleavage. In case of lysozyme, even the denatured protein is cleaved by Py-Phe, indicating such access is attainable even in the denatured state (data not shown), or that the protein renatures quickly, prior to photoactivation.

3.6 *Quenching of protein cleavage reaction by oxygen, ethanol, and ethanolamine*

Quenching of Py-Phe* by CoHA results in the formation of the corresponding cation radical ($Py^{+\bullet}$), and this was verified in flash photolysis studies.[3] Further insights into the details of the photocleavage are obtained from mechanistic studies involving quenching by oxygen, ethanol, and ethanolamine. Singlet oxygen is not responsible for the observed photocleavage, because irradiation in the presence of Py-Phe but in the absence of CoHA did not result in cleavage (figure 5a, lane 5). Azide, known singlet oxygen quencher, does not inhibit the reaction. However, oxygen is important for the BSA cleavage, and the effect of oxygen concentration on photocleavage yields is shown in figure 6a. Degassing the reaction mixture prior to irradiation suppressed BSA cleavage (figure 6a, lane 4), indicating the key role of oxygen in the cleavage reaction. When the reaction mixture was saturated with oxygen, BSA cleavage is suppressed (figure 6a, lane 5). Oxygen is

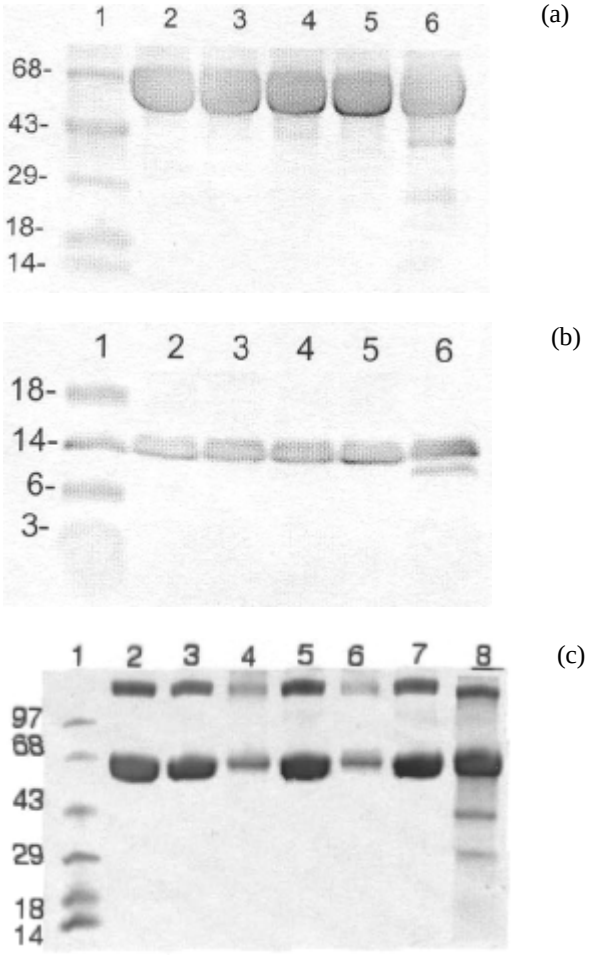

Figure 5. (**a**) Gel electrophoresis pattern of attempted photoreaction of BSA with the methyl ester of Py-Phe (Py-Phe-Me). Lane 1: molecular weight markers, indicated in kilodaltons; lane 2: BSA (15 *m*M), Py-Phe-Me (5 *m*M), CoHA (0·33 mM), dark control; lanes 3, 4: same as lane 2, but irradiated for 15 and 30 min at 350 nm respectively; lane 5: BSA (15 *m*M), Py-Phe-Me (5 *m*M) irradiated for 30 min; and lane 6: BSA (15 *m*M), Py-Phe (5 *m*M), CoHA (0·33 mM) irradiated for 15 min at 344 nm; (**b**) Gel electrophoresis pattern of attempted photoreaction of lysozyme with the methyl ester of Py-Phe (Py-Phe-Me). Lane 1: molecular weight markers, indicated in kilodaltons; lane 2: lysozyme (15 *m*M), Py-Phe-Me (5 *m*M), CoHA (0·33 mM); lanes 3, 4: same as lane 2, but irradiated for 5 and 10 min at 350 nm respectively; lane 5: lysozyme (15 *m*M), Py-Phe-Me (5 *m*M) irradiated for 10 min; and lane 6: lysozyme (15 *m*M), Py-Phe (5 *m*M), CoHA (0·33 mM), irradiated for 5 min at 344 nm; (**c**) Attempted photocleavage of BSA after heat denaturation. Lane 1: molecular weight markers, indicated in kilodaltons; lane 2: heat denatured BSA (15 *m*M); lane 3: heat denatured BSA (15 *m*M), Py-Phe (15 *m*M), CoHA (1 mM); lane 4: same as lane 3, but irradiated for 40 min at 344 nm; and lane 5: 15 *m*M denatured BSA irradiated for 40 min; lane 6: 15 *m*M denatured BSA + 15 *m*M Py-Phe irradiated for 40 min; lane 7: 15 *m*M denatured BSA, 1 mM CoHA, irradiated for 40 min, 8: 15 *m*M BSA + 15 *m*M Py-Phe + 1 mM CoHa, irradiated for 40 min.

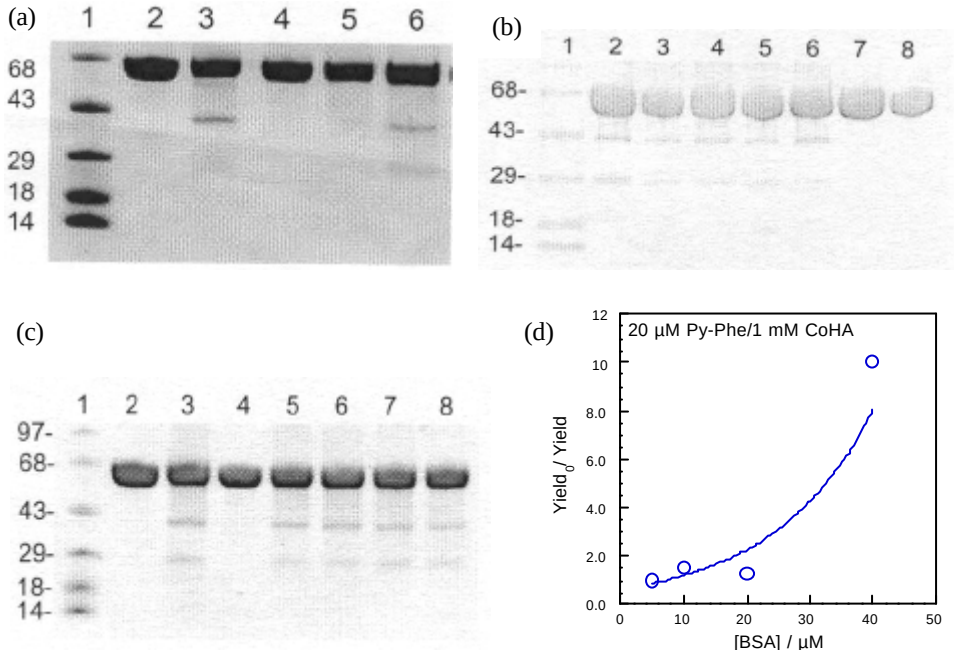

Figure 6. (**a**) Effect of oxygen on the photocleavage of BSA. Lane 1: molecular weight markers, indicated in kilodaltons; lane 2: BSA (15 *m*M), Py-Phe (15 *m*M) and CoHA (1 mM) not exposed to light; lane 3: same as lane 2 but after irradiation at 344 nm for 40 min; lane 4: same as lane 3 but degassed by bubbling with nitrogen for 40 min prior to irradiation; lane 5: same as lane 3 solution was bubbled with oxygen for 40 min prior to irradiation; lane 6: same as lane 3; (**b**) Quenching of the photocleavage of BSA by increasing concentrations of ethanol. Lane 1: molecular weight markers, indicated in kilodaltons; lane 2: BSA (15 *m*M) Py-Phe (15 *m*M) and CoHA (1 mM) after irradiation at 344 nm for 10 min; Lanes 3–6; Lane 3: BSA (15 *m*); are the same as lane 2 but irradiated in the presence of 0·05, 0·1, 0·15, and 0·2 M ethanol respectively. Lane 7: same as lane 6 but not exposed to light; lane 8: BSA (15 *m*M), Py-Phe (15 *m*M), 0·2 M EtOH, after irradiation at 344 nm for 10 min; (**c**) Quenching of the photocleavage of BSA by increasing concentrations of ethanolamine. Lane 1: molecular weight markers, indicated in kilodaltons; lane 2: BSA (15 *m*M); Lane 3: BSA (15 *m*M), Py-Phe (15 *m*M) and CoHA (1 mM) after irradiation at 344 nm for 40 min; lane 4: BSA (15 *m*M), Py-Phe (15 *m*M) and CoHA (1 mM), ethanolamine (1 mM); lanes 5–8 are the same as lane 3 but irradiated for 40 min at 344 nm in the presence of 1, 2, 3, and 5 mM ethanolamine respectively. Note that lane 4 is the same as lane 8 but not exposed to 344 nm light; (**d**) Quenching of protein cleavage by BSA. The ratio of yield at 5 *m*M BSA to that at higher BSA concentration is plotted as a function of BSA concentration.

essential for BSA cleavage, but high concentrations of oxygen quenches Py* in competition with CoHA, and this results in the inhibition of photocleavage.

The participation of other radical intermediates in the photocleavage is tested in quenching studies with ethanol (figure 6b). Ethanol quenches hydroxyl radicals at diffusion controlled rates,[31] and reacts with carbon centered radicals at much slower rates. The photocleavage of BSA is quenched by ethanol (0–0·2 M), as shown in figure 6c (lanes 2–6), and the data suggest that radical intermediates other than $Py^{+\bullet}$ are also involved.

Quenching of $Py^{+\bullet}$ by ethanol can not be ruled out, and this possibility will be tested in future experiments.

To correlate the detection of $Py^{+\bullet}$ in the tie-resolved experiments with the steady state data, we tested the interception of $Py^{+\bullet}$ with ethanolamine in steady state experiments. Consistent with this expectation, irradiation in the presence of increasing concentrations of ethanolamine (0–5 mM) inhibited the photocleavage (figure 6c, lanes 3, 5–8). Taken together, the data indicate that $Py^{+\bullet}$ is indeed a key intermediate in the observed protein cleavage. The photocleavage of BSA, therefore, is inhibited by heat denaturation, oxygen, ethanolamine, and ethanol, but not by azide.

The photocleavage yields depended on the concentration of Py-Phe, BSA and CoHA, and the yield is quenched by BSA (figure 6d). A plot of the ratio of cleavage yield at 5 μM BSA to yield at higher BSA concentrations shows an upward curvature (BSA concentration 5–40 μM, 1 mM CoHA, 20 μM P-Phe) and such upward curvature is typical for static quenching. The observed quenching is most likely due to protein-protein interactions, and/or quenching of long-lived radical intermediates by BSA.[32] Yields are better at lower BSA concentrations.

4. Discussion

4.1 *Spectral studies*

The presence of two distinct binding sites for Py-Phe on BSA is indicated from figure 1a. The two binding plots (open and closed circles) overlap at low BSA concentrations, but deviate at high concentrations. At low concentrations, therefore, both sites are occupied, and binding results in the rapid loss of absorbance at 343 nm. At BSA concentrations >1:1 stoichiometry (protein to ligand), the binding equilibrium favors the thermodynamically favorable site with concomitant increase in the absorbance at 347 nm. Binding to the low affinity site, therefore, lowers the extinction coefficient with no detectable change in peak positions, but binding to the high affinity site results in a red-shift with increase in absorbance at 347 nm. Decreased extinction coefficients are observed when Py-Phe binds to lysozyme (table 1), and the low affinity site in BSA shares some features of that in lysozyme.

The fluorescence spectra of the lysozyme-bound Py-Phe indicate no excimer emission, and hence, the probe exists as a monomer at the binding site. The spectra are shifted by 2 nm, when compared to that of the free probe, and the Stokes shift for the BSA-bound probe is much smaller than that in lysozyme or buffer. The reduced Stoke's shift is indicative of the rigidity of the medium surrounding the probe in BSA, and this conclusion is consistent with our previous observation that Py-Phe in lysozyme is exposed to the solvent but not Py-Phe bound to BSA.[3] The solvent access to the binding sites is further differentiated in fluorescence quenching studies.

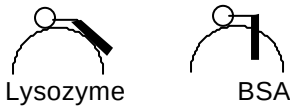

Chart 5. Binding of the Py group on the exterior of lysozyme while it is buried deeply in BSA, as indicated from the time-resolved fluorescence quenching studies.

CoHA quenches Py-Phe fluorescence at diffusion-controlled rates (table 1), and this rate is reduced when it binds to lysozyme, but little or no quenching is detected when bound to BSA. Steady-state quenching studies reported earlier,[3] did not distinguish between the static and dynamic components of quenching. The quenching rate constants obtained in the time-resolved studies reported here, agree with the earlier steady state data (Ksv = kq.τ). The quenching observed for lysozyme in steady state experiments, therefore, is mostly due to collisional quenching while that of BSA is due to static quenching. The large value of the quenching rate constant observed with Py-Phe/ lysozyme confirms the facile access of the probe to CoHA, and access is severely restricted in case of BSA (chart 5). This conclusion is also consistent with the strong ICD spectrum observed with BSA, while that of lysozyme is more similar to that of the free probe (figure 4).

4.2 *Photocleavage studies*

The pyrenyl excited state (Py*), by itself, does not cause protein cleavage. Our goal has been to use Py* to generate radical intermediates in the protein matrix, and induce protein cleavage at the probe binding site. Generation of $Py^{+\bullet}$ via quenching of the Py* by CoHA, results in facile cleavage of BSA/lysozyme with specificity.[3] Protein sequencing studies of the resulting peptide fragments indicate that the carboxylate function of the probe may be involved in salt-bridge formation with Arg residues at the binding sites on BSA and lysozyme. To investigate this possibility, we have tested the photoreactivity of the methyl ester of Py-Phe and the methyl ester does not cleave either BSA or lysozyme (figure 5a, b). Therefore, the COOH group is essential for the recognition and specificity of photocleavage.

The availability of specific reactive sites on the protein is also essential for the observed reactivity. The denatured BSA is not cleaved by Py-Phe, a clear indication that the native structure of BSA is essential for the reaction (figure 5c). Thus, a combination of recognition by the probe, as well as reactivity of specific sites on the protein form the basis for the observed specificity.

4.3 *Quenching studies*

Quenching of Py-Phe* by oxygen is expected to generate singlet oxygen, and it is known to cause damage to proteins and DNA. But, singlet oxygen is not involved in the current reactions as CoHA is essential for the reaction, saturation of the reaction mixture with oxygen suppressed product formation, and azide does not quench the photoreaction (figure 6a).

The participation of long-lived radical intermediates in the photoreaction is indicated from quenching experiments with ethanol (figure 6b). The interception of the short-lived hydroxyl radical (lifetime < 10 ns) requires higher concentrations of ethanol than used here, and current data indicate that ethanol is intercepting long-lived radicals but not the hydroxy radical.

Quenching of Py-Phe* by CoHA results in the formation of $Py^{+\bullet}$ as reported previously, and current studies support the key role of the cation radical in the photoreaction. Product yield is quenched by electron donors such as ethanolamine with a quenching constant of 60 M^{-1} (figure 6c). The long lifetime of $Py^{+\bullet}$ (~ 50 μs)[3] allows us to intercept this intermediate without affecting the much shorter lived Py* (τ_f = 110 ns). The rate

constant, k_a, for the quenching of $Py^{+\bullet}$ by ethanolamine is $1{\cdot}3 \times 10^6\ M^{-1}\ s^{-1}$, and this value agrees well with the Stern-Volmer constant (K_{sv}) of 60 M^{-1} ($K_{sv} = kq^* \boldsymbol{t}$), estimated from the steady state data. This correlation indicates that $Py^{+\bullet}$ is the key intermediate leading to the protein cleavage. The protein cleavage is also quenched by BSA (figure 6d), and the data clearly indicate the dominance of protein–protein interactions at high concentrations. The quenching data, therefore, rule out the possibility of singlet oxygen or the hydroxyl radical as the source of the observed photocleavage, and it involves long-lived radicals whose reactivity is sensitive to protein conformation.

Current results clearly indicate a single cut in the protein backbone and hence, 100% selectivity or specificity for the photoreaction. Photocleavage studies when coupled to mechanistic investigations will be in the rational design of chemical reagents to target specific sites of proteins. In addition to biochemical applications, such reagents may be of interest for therapeutic purposes.

5. Conclusions

Binding of ligands to proteins at specific sites, and their activation to induce protein cleavage with specificity (100% selectivity) is demonstrated. Binding is controlled by arranging specific functional groups at desired locations on the probe, while the cleavage yield is controlled by the availability of specific reactive sites on the protein. These distinct aspects work together to result in the observed specificity.

Acknowledgements

We are grateful for financial support from the University of Connecticut Research Foundation, NSF (DMR-9729178), and the donors of the Petroleum Research Fund (PRF 33821-AC4).

References

1. Suckling C J 1990 *Enzyme chemistry: Impact and applications* 2nd edn (London: Chapman and Hall)
2. Kumar C V and Buranaprapuk A 1997 *Angew. Chem., Int. Ed. Engl.* **36** 2085
3. Kumar C V, Buranaprapuk A, Opiteck G J, Moyer M B, Jockusch S and Turro N J 1998 *Proc. Natl. Acad. Sci. USA* **95** 10361
4. Kumar C V and Buranaprapuk A 1999 *J. Am. Chem. Soc*. **121** 4262
5. Buranaprapuk A, Kumar C V, Steffen J and Turro N J 2001 *Tetrahedron* **56** 7019
6. Kumar C V, Buranaprapuk A and Sze H C 2001 *Chem. Commun*. 297
7. Rana T M and Meares C F 1991 *J. Am. Chem. Soc.* **113** 1859
8. Rana T M and Meares C F 1991 *Proc. Natl. Acad. Sci. USA* **88** 10578
9. Rana T M and Meares C F 1990 *J. Am. Chem. Soc*. **112** 2457
10. Ghaim J B, Greiner D P, Meares C F and Gennis R B 1995 *Biochemistry* **34** 11311
11. Ettner N, Ellestad G A and Hillen W 1993 *J. Am. Chem. Soc*. **115** 2546
12. Ettner N, Metzger J W, Lederer T, Hulmes J D, Kisker C, Hinrichs W, Ellestad G and Hillen W 1995 *Biochemistry* **34** 22
13. Krotz A H, Kuo L Y, Shields T P and Barton J K 1993 *J. Am. Chem. Soc*. **115** 3877
14. Gupta N, Grover N, Neyhart G A, Singh P and Thorp H H 1993 *Inorg. Chem*. **32** 310
15. Cremo C R, Loo J A, Edmonds C G and Hatlelid K M 1992 *Biochemistry* **31** 491
16. Crans D C, Sudhakar K and Zamborelli T 1992 *Biochemistry* **31** 6812
17. Schepartz A and Cuenoud B 1990 *J. Am. Chem. Soc.* **112** 3247
18. Cuenoud B, Tarasow T M and Schepartz A 1992 *Tetrahedron Lett.* **33** 895
19. Hoyer D, Cho H and Schultz P G 1990 *J. Am. Chem. Soc*. **112** 3249

20. Ermacora M R, Delfino J M, Cuenoud B, Schepartz A and Fox R O 1992 *Proc. Natl. Acad. Sci. USA* **89** 6383
21. Muirhead H 1979 *Int. Rev. Biochem.* **24** 37
22. Gelamo E L, Silva C H T P, Imasato H and Tabak M 2001 *Biochim. Biophys. Acta* **1594** 84
23. Kumar C V, Buranaprapuk A, Cho A and Chaudhari A 2000 *Chem. Commun.* 597
24. Goldstein F B 1963 *Biochim. Phiophys. Acta* **71** 204
25. Blake C C F, Koenig D F, Mair G A, North A C T, Phillips D C and Sarma V R 1965 *Nature* (*London*) **206** 757
26. Jones M N, Skinner H A and Tipping E 1975 *Biochem. J.* **147** 229
27. Schägger H and von Jagow G 1987 *Anal. Biochem.* **166** 368
28. Kumar C V and Tolosa L M 1993 *J. Phys. Chem.* **97** 13914
29. Kumar, C V and Tolosa L M 1993 *FASEB J.* **7** A1131
30. Kumar C V and Asuncion E H 1993 *J. Am. Chem. Soc.* **115** 8547
31. Sankarapandi S and Zweier J L 1999 *J. Biol. Chem.* **274** 34576
32. Roberfriod M and Calderon P B 1995 in *Free radicals and oxidation phenomena in biological systems* (New York: Marcel Dekker) pp 114–115